The ISME Journal (2019) 13:1639–1646
https://doi.org/10.1038/s41396-019-0369-0

ARTICLE

Visualizing the dynamics of soil aggregation as affected by arbuscular mycorrhizal fungi

E. K. Morris[1,2] · D. J. P. Morris[3] · S. Vogt[4] · S.-C. Gleber[4,5] · M. Bigalke[6] · W. Wilcke[7] · M. C. Rillig[2]

Received: 26 September 2018 / Revised: 30 December 2018 / Accepted: 19 January 2019 / Published online: 11 February 2019

Abstract

Stable soils provide valuable ecosystem services and mechanical soil stability is enhanced by the presence of arbuscular mycorrhizal fungi (AMF). Soil aggregation, which is the major driver of mechanical soil stability, is often treated as a static phenomenon, even though aggregate turnover is continually ongoing. In fact, some breakdown of macroaggregates is necessary to allow new aggregate formation and inclusion of new organic matter into microaggregates. We determined how aggregate turnover times were affected by AMF by tracking movement of rare earth elements (REE), applied as their immobile oxides, between aggregate size classes, and using X-ray fluorescence microscopy to spatially localize REEs in a sample of aggregates. Here we show that AMF increased large macroaggregate formation and slowed down disintegration of large and small macroaggregates. Microaggregate turnover was increased in the presence of AMF. Internal aggregate organization suggested that although formation of microaggregates by accretion of soil to particulate organic matter is common, it is not the only mechanism in operation.

Introduction

Soil structure is a crucial ecosystem service important for maintaining soil porosity, gas exchange, water infiltration, erosion resistance, and carbon sequestration [1–6]. Soil aggregates, clusters of soil particles that adhere to each other more strongly than to surrounding particles, are one component of soil structure. Microbial activity is limited within the aggregates, allowing 0.4−1.2 Pg carbon to be sequestered globally each year in soil aggregates [2, 7–9].

Though often assessed as a static phenomenon, soil aggregates are constantly formed and degraded at temporal scales that can be as short as a few weeks [10]. Aggregate turnover times have important consequences for carbon sequestration by soils because the incorporation of carbon into aggregates protects it from being quickly released as CO_2 into the atmosphere by mineralization [6]. Aggregate formation is hypothesized to occur as follows. In soils containing organic matter, macroaggregates (>250 µm diameter) appear as primary particles (<53 µm diameter) held together by transient binding agents such as roots, hyphae, and polysaccharides. Microaggregates (53–250 µm diameter) form within macroaggregates (or freely) when transient binding agents become encrusted with clays, limiting access to organic matter within the microaggregate and slowing further decomposition [6, 11]. As transient binding

Supplementary information The online version of this article (https://doi.org/10.1038/s41396-019-0369-0) contains supplementary material, which is available to authorized users.

✉ E. K. Morris
morrisk10@xavier.edu

1 Department of Biology, Xavier University, 3800 Victory Parkway, Cincinnati, OH 45207, USA

2 Institut für Biologie, Pflanzenökologie, Freie Universität Berlin, Altensteinstr. 6, 14195 Berlin, Germany

3 Department of Physics, Xavier University, 3800 Victory Parkway, Cincinnati, OH 45207, USA

4 Advanced Photon Source, Argonne National Laboratory, 9700 South Cass Ave., Lemont, IL 60439, USA

5 Institut für Röntgenphysik, Georg-August-Universität Göttingen, Friedrich-Hund-Platz 1, 37077 Göttingen, Germany

6 Institute of Geography, University of Bern, Hallerstrasse 12, 3012 Bern, Switzerland

7 Institut für Geographie und Geoökologie, Karlsruher Institut für Technologie (KIT), Reinhard-Baumeister-Platz 1, 76131 Karlsruhe, Germany

agents decompose, or if a disturbance occurs, microaggregates are released and slowly break down to primary particles [4, 12].

This process is dynamic, and some breakdown of macroaggregates is necessary to allow inclusion of incoming labile organic matter into new microaggregates [13] and macroaggregates [14]. Soils with extremely long aggregate turnover times sequester little new carbon but stabilize the carbon in their interior for long times, while extremely short turnover times can potentially sequester a lot of new carbon but could also reduce overall soil stability if aggregates are not regenerated at the same rate that they degrade [12]. If a management change aims at increasing carbon sequestration, aggregate turnover times somewhere in between these extremes might be desirable to maintain soil stability and sequester new carbon, while also seeing improvements in other ecosystem services associated with soil stability.

Biotic factors play a key role in soil stability, and fungal hyphae, especially those produced by arbuscular mycorrhizal fungi (AMF), are among the most important factors affecting long-term soil aggregation [5, 15–22]. Much of the aggregating capacity of fungi is attributed to their filamentous growth habit giving the ability to enmesh particles in soil [5, 23]. We therefore expect AMF to be especially important for macroaggregate formation, but to not have a direct impact on microaggregate turnover dynamics since microaggregate dynamics are hypothesized to be much less affected by plant and fungal enmeshing.

Here we use rare earth elements (REE) as tracers to quantify the turnover of aggregates in a selected arable soil deemed representative for large parts of Central European arable soils with and without AMF [24–26], along with X-ray fluorescence microscopy [27, 28] to localize REEs and other elements within select aggregates. We prepared REE-labeled soil with each of four size classes labeled with a different REE (added as oxides), and reassembled those four labeled size classes into a highly aggregated composite soil so that we could track aggregate turnover dynamics. We then incubated that soil, in hyphal in-growth cores that prevented access by plant roots, with and without AMF ($N = 3$) in pots with *Plantago lanceolata* for 5 weeks, a time period expected to allow for both growth of AMF hyphae throughout soil [29] and for observation of initial turnover events [26]. After harvesting and sieving soil into four size classes we digested samples with strong acids and used ICP-MS to quantify REEs in each size class, and then calculated turnover between the four size classes, and combined that with high resolution maps of internal aggregate structure obtained at the Advanced Photon Source at Argonne National Laboratory to compare theoretical predictions of mechanisms of aggregate formation and structure [4, 30].

AMF stabilize large macroaggregates

Large macroaggregates were more abundant in the presence of AMF while microaggregates and primary particles declined (Supplementary Table 1, Fig. 1a). Small macroaggregates made up about 15% of the total soil mass in both treatments, and were not affected by AMF presence.

Without AMF, about a quarter of each of the three smallest size classes was incorporated into large macroaggregates during the 5-week incubation period, while about half of the macroaggregates present at the start of the experiment broke down during the experiment (Table 1, Supplementary Table 2, Fig. 1b). With AMF, just over half of each of the three smallest size classes was incorporated into large macroaggregates during the experiment, while only 27% of the existing large macroaggregates broke down during the course of the experiment. Overall, pathways creating large macroaggregates were about twice as active with AMF than without, while those degrading large macroaggregates were only half as active with AMF than without, emphasizing the stabilizing effect of AMF on large macroaggregates.

Aggregate turnover

We observed the longest turnover times in the largest aggregates especially if AMF were present, while other studies reporting aggregate turnover times in various aggregate classes have all observed the longest aggregate turnover times in the smallest aggregates [24, 26, 31]. The soils used in the earlier studies may have contained saprobic fungi and bacteria, but they did not contain plant roots or AMF, and it is not surprising that macroaggregates were less stable without the presence of such key factors in macroaggregate formation and stabilization. The stabilizing effect of AMF on macroaggregates is apparent in the longer turnover times of macroaggregates seen in our study, a phenomenon predicted elsewhere [12]. Plant roots and fungal hyphae together have a greater aggregating effect than fungal hyphae alone [15, 32], and our experimental soil only contained hyphae. Our results, therefore, probably underestimate the potential of roots and hyphae to contribute to macroaggregate formation and stabilization, and therefore underestimate the potential for C stabilization in microaggregates.

AMF likely contribute to carbon stabilization primarily by increasing the stability of macroaggregates. This would allow for direct carbon stabilization within macroaggregates, and for enhanced production of microaggregates which would stabilize more carbon [6]. We did not observe a direct stabilization effect of AMF on microaggregates, but many microaggregates likely form within

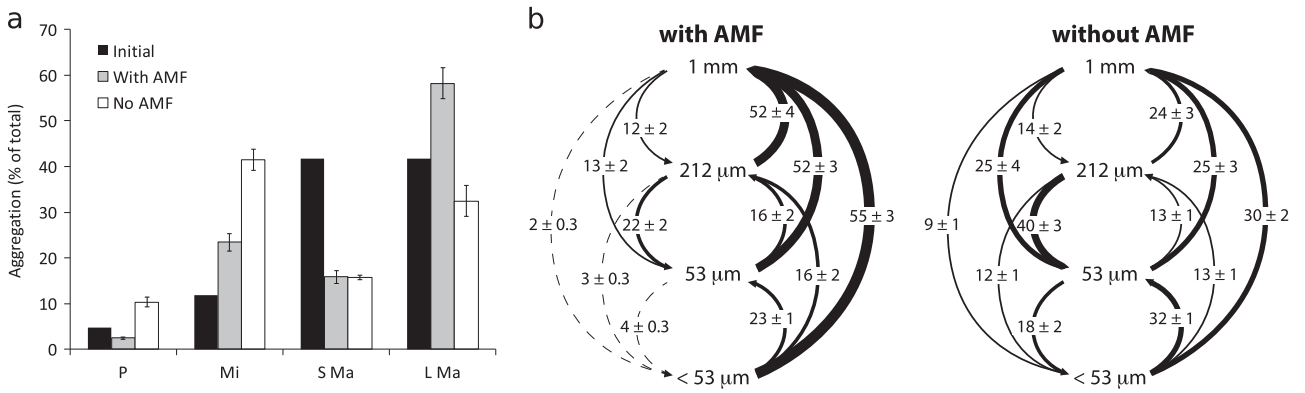

Fig. 1 Aggregate size class distributions (**a**) and transformation pathways, percentage of the original size class that is transformed into the new size class (**b**) (mean ± SE, $N = 3$) in soils incubated with or without AMF for five weeks. L Ma—large macroaggregates (1–2 mm), S Ma—small macroaggregates (212–1000 µm), Mi—microaggregates (53–212 µm), P—primary particles (<53 µm). **a** Initial—Size class distribution before treatments were applied. **b** Solid lines indicate significant differences between soils with and without AMF, while dashed lines indicated nonsignificant differences. Line thickness represents magnitude of the transformation pathway

Table 1 Data and statistical analysis of the effects of AMF on aggregate turnover times

Turnover time	Without AMF (d) (Mean ± SE)	With AMF (d) (Mean ± SE)	F (df = 1,4)	*p*
Large macroaggregates (1–4 mm)	76 ± 10	139 ± 20	7.9	0.0485
Small macroaggregates (0.212–1 mm)	46 ± 1.2	46 ± 1.0	0.2	0.6785
Microaggregates (53–212 µm)	63 ± 1.6	49 ± 0.94	58	0.0016
Particles (<53 µm)	47 ± 1.2	37 ± 0.20	56	0.0017

AMF arbuscular mycorrhizal fungi

macroaggregates [4], and the short time course of our experiment was selected to capture initial transformation events (i.e., particles into macroaggregates or macroaggregates into microaggregates), so from our data we cannot shed light on longer term transformation events. The faster turnover of macroaggregates seen without AMF suggests that fewer microaggregates will be formed within the macroaggregates in those soils, and that less C will be stabilized in soils without AMF [9, 33, 34].

Aggregate spatial structure

The X-ray fluorescence data provided qualitative snapshots of eight aggregate thin sections at the end of the 5-week REE incubation period (Fig. 2, Supplementary Figures 1–8). We were only able to examine a small number of aggregates due to the time-consuming nature of the technique, so X-ray fluorescence data were used to provide insight into mechanisms operating during aggregate turnover of the same soil samples that were precisely quantified using ICP-MS data. At the start of the experiment, large macroaggregates were labeled with gadolinium (Gd), small macroaggregates were labeled with samarium (Sm), microaggregates were labeled with neodymium (Nd), and primary particles were labeled with lanthanum (La). Based on REE distribution in the thin sections, we were able to identify which size classes each part of each aggregate originated from. For example, soil clumps containing Gd must have originated from the large macroaggregates that were labeled with Gd at the start of incubation.

The X-ray fluorescence data indicated that the small macroaggregate incubated with AMF remained intact throughout the incubation period (Fig. 2—Agg D). Of the three microaggregates incubated with AMF, two were fragments of small macroaggregates (Fig. 2—Aggs A, C) and one of these (Agg A) contained a V-shaped cavity (Supplementary Figure 9a) that did not contain any of the other elements that we could detect using X-ray fluorescence (Si, P, S, Cl, Ar, K, Ca, Ti, Cr, Mn, Fe, Co, Ni, Cu, Zn, REEs; Supplementary Figure 1). Since organic matter would contain many of these elements it is likely that the cavity is a true void. The third microaggregate incubated with AMF was formed from primary particles during incubation while incorporating bits of fully broken down small macroaggregates (Fig. 2—Agg B).

Based on the X-ray fluorescence data, the small macroaggregate incubated without AMF formed from fragments of small macroaggregates and microaggregates and contained a void that was filled with primary particles during

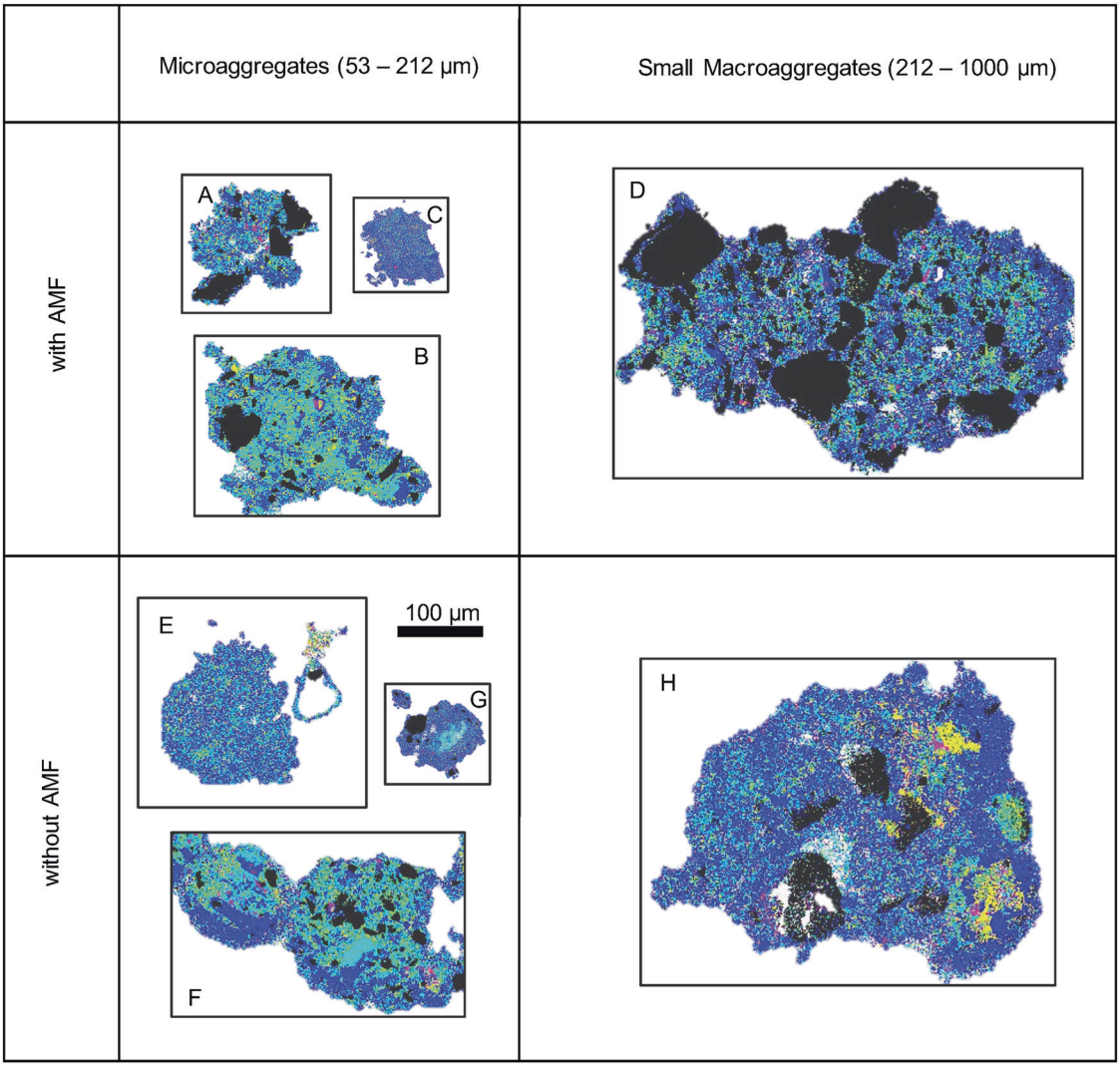

Fig. 2 X-ray fluorescence data for a sample of aggregates. Images show locations of five elements in each aggregate thin section. Each pixel, the finest unit of resolution during microscopy, is drawn with only one color representing either a sand grain if present, or the most abundant REE in that pixel. Sand grains are seen as Si—black. At the start of the experiment large macroaggregates were labeled with Nd—yellow, small macroaggregates were labeled with Sm—blue, microaggregates were labeled with Gd—magenta, and primary particles were labeled with La—cyan

incubation (Figs. 2, 3—Agg H). The three microaggregates incubated without AMF demonstrated the same three formation mechanisms observed in soils with AMF. Two microaggregates were fragments of small macroaggregates (Fig. 2—Aggs E, G), and one of those contained a void that was filled with primary particles during incubation (Agg G). We also observed a fragment of a microaggregate (Fig. 2—near Agg E) and a soil encrusted triangular void that was either a fragment of small macroaggregate or encrusted with soil from broken down small macroaggregates (Fig. 2—near Agg E). The final microaggregate incubated without AMF was likely formed by accretion of primary particles and broken down small macroaggregates onto concave shells remaining after fracturing of a small macroaggregate along internal voids (Figs. 2, 3—Agg F, Supplementary Figure 9).

Macroaggregates are expected to benefit more from the presence of AMF than do microaggregates [5, 16], so it is not surprising that the microaggregates observed were similar regardless of whether they were incubated with or without AMF.

We observed voids, which although empty at the end of the experiment, may have originally been filled with organic matter as predicted by Tisdall [30]. She suggested that microaggregates would consist of plant or fungal fragments surrounded by soil crusts (>100 µm), or be empty after the organic matter centers had degraded (<90 µm). In contrast, Vogel showed that organic matter preferentially binds to

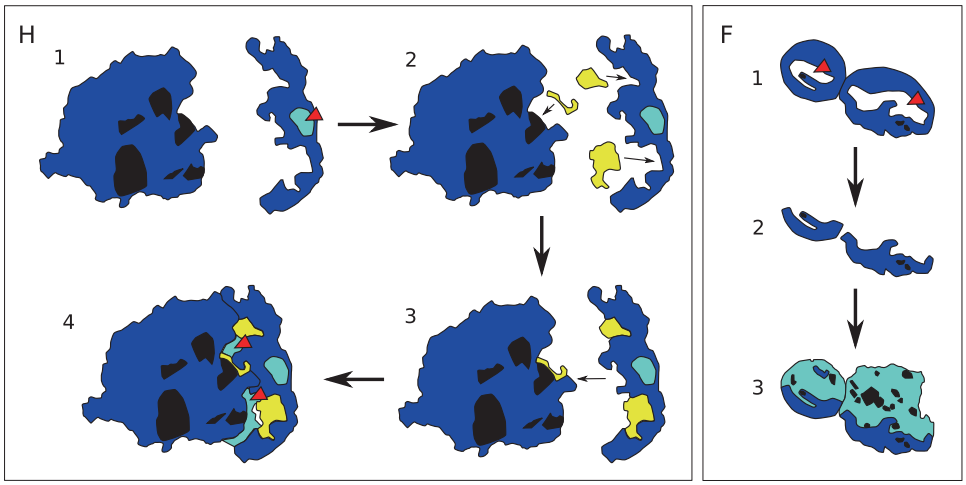

Fig. 3 Proposed aggregate formation mechanisms. Si—black, Sm—blue, Nd—yellow, La—cyan. Aggregate H. Step 1: On the left one existing small macroaggregate, or a fragment of one, contains six sand grains. On the right a fragment of a small macroaggregate contains a void that is filled with La-labeled primary particles and a K-containing substance (red arrowhead). Step 2: Fragments of Nd-labeled microaggregates fuse to existing Sm-labeled soil. Step 3: The two Sm-labeled aggregates fuse. Step 4: Gaps created during fusion fill with La-labeled primary particles (red arrowheads). Aggregate F. Step 1: Existing small macroaggregates have internal voids (red arrowheads). Step 2: Those small macroaggregates fracture along void edges, leaving two concave edges. Step 3: Accretion of primary particles and degraded larger aggregates to concave edges forms new small macroaggregates

other organic matter, even on aggregate surfaces [35]. We could not visualize C with our X-ray fluorescence technique, but we observed aggregates with voids matching Tisdall's description (A, E, G; Fig. 2), and some without voids matching the description of Vogel et al. (B, C, E, F; Fig. 2). Our soil aggregates formed initially in soils without plants and fungal hyphae, so large organic structures (e.g., roots and fungi) were not abundant, but we did add chopped *Festuca* leaves at the start of aggregate formation, so there was particulate organic matter for microaggregates to form around.

Conclusions

AMF increase stability of soil macroaggregates, a key contributing factor to the many ecosystem services provided by AMF (e.g., carbon sequestration, gas exchange, water infiltration, and erosion resistance). The presence of plant roots, soil type, moisture, and organic matter content also impact the percent of aggregated soil in a sample [15, 36, 37], and likely also turnover times, but monitoring effects of such factors was outside the scope of this work. AMF consistently enhance soil aggregation across soil types [5], so it is likely that the AMF effects on aggregate turnover that we identified are also consistent across soil types, although absolute turnover rates likely vary with other abiotic and biotic factors.

Among the aggregates that we visualized with an element sensitive imaging technique, it was clear that one mechanism of aggregate formation was not dominant. In fact, we observed the same variety of spatial arrangements of microaggregates and small macroaggregates regardless of AMF treatment. This reinforces the view that AMF are more important for large macroaggregate formation and stability.

Methods

Experimental design

We grew *P. lanceolata* L. in steamed topsoil (60 °C for 30 min), collected from the agricultural experimental station of the Humboldt University in the metropolitan area of Berlin. The soil, an Albic Luvisol [38], had the following properties: 73.6% sand, 18.8% silt, 7.6% clay; pH 7.1 ($CaCl_2$); 1.87% C (total); C/N—15.58 (analyses conducted by LUFA Rostock Agricultural Analysis and Research Institute, Germany; and on a Euro EA C/N analyzer, HEKAtech GmbH, Wegberg, Germany). Plants were grown in 2-L pots, each containing a 5 cm diameter hyphal in-growth core (HIGC) prepared by wrapping a plastic filter cylinder with 30 µm mesh (Sefar Nitex 03-30/18, Sefar GmbH, Edling, Germany) that would contain a sample of REE-amended soil that could not be accessed by plant roots. This allowed us to focus on effects of AMF, which produce hyphae fine enough to easily enter the HIGCs. Ten pots were set up, five with AMF and five without. Two of the five replicates in the treatment with AMF were eventually

excluded because they had very low levels of colonization, leaving $N = 3$. Two of the five replicates in the treatment without AMF were also eventually excluded because they had non-zero low levels of AMF colonization, leaving $N = 3$. AMF inoculum was prepared from *Festuca rubra* L. plants grown in a field plot in Berlin, Germany by chopping fresh AMF containing roots into segments approximately 1 cm long. Control pots received autoclaved (121 °C for 15 min) AMF inoculum. Pots were filled with steamed soil, and then 10 g of inoculum were placed on the surface of the soil. *P. lanceolata* seeds were surface sterilized in 20% bleach for 5 min, and then rinsed thoroughly before placing on top of the inoculum. Inoculum and seeds were covered with a 1 cm layer of steamed soil, and placed in a greenhouse with ambient light.

REE-labeling of soil

REE-labeled soil was prepared also using soil collected from the Humboldt University site. After air drying it at room temperature, dry soil was passed through a 2 mm sieve to remove large coarse particles and particulate organic matter, then tumbled in a cement mixer with paving stones (average diameter 6 cm) for 30 min to crush the soil. Only crushed soil that passed through a 53 µm sieve was retained. Crushed soil was steamed (60 °C for 30 min) to kill AMF, then split into four separate batches and combined with either lanthanum oxide (La_2O_3), neodymium oxide (Nd_2O_3), samarium oxide (Sm_2O_3), or gadolinium oxide (Gd_2O_3) at 300 mg of the respective oxide kg^{-1} soil. Organic matter was supplied as autoclaved (121 °C for 15 min) finely chopped *F. rubra* leaves (1.5% of soil mass), and then soil was watered to 65% field capacity. Soil was incubated in closed containers at room temperature for 4 weeks, then air-dried at room temperature. Dried soil was dry sieved to separate into four size classes: large macroaggregates (1–4 mm), small macroaggregates (212 µm−1 mm), microaggregates (53–212 µm), and smaller particles (<53 µm).

An experimental REE-labeled soil was created by mixing the four individual REE-labeled aggregate size classes to obtain a soil that was 41.8% large macroaggregates labeled with Nd_2O_3, 41.8% small macroaggregates labeled with Sm_2O_3, 11.6% microaggregates labeled with Gd_2O_3, and 4.8% smaller particles labeled with La_2O_3. This distribution was chosen to represent a highly aggregated soil typical of managed grasslands in Germany [15].

REE incubation

The HIGCs in the pots for the first 2 months were empty, and served as placeholders for the REE-labeled soil containing HIGCs that were then placed in pots for an additional 5 weeks of growth. Pots were given the initial 2 months to establish fungal networks throughout the pot before the REE phase of the experiment. Once the REE-containing HIGCs were placed in pots, existing fungal networks would have quickly colonized the HIGCs. After incubation, the REE-containing HIGCs were removed from pots and the soil within was spread thinly to air dry at room temperature. *P. lanceolata* plants were harvested, and the roots were preserved in 50% ethanol until verification of AMF colonization. Roots were cleared in 10% KOH, stained in 10% India ink (Sheaffer Pen, Middlesex, UK) in 5% acetic acid, then destained in lactoglycerol [39]. Stained roots were mounted in glycerol and examined at ×200 magnification for the presence of mycorrhizal fungal structures [40].

Soil processing

Air-dried soil was dry sieved to separate the soil into the same four aggregate size classes used when preparing the initial soil. We chose dry sieving over the standard wet-sieving method for two reasons. First, we wanted to minimize the chances of REE leaching from aggregates during wet sieving and confounding results. Second, we needed dry intact aggregates for the X-ray fluorescence imaging, and were concerned that wet sieving followed by drying would both introduce artifacts and make it difficult to isolate individual intact aggregates. Others have used dry sieving and found relatively similar results to wet sieving, although dry sieving can produce higher MWD because aggregates are not subjected to the disintegrating force of water [41]. REEs were extracted from a sample of aggregates from each size class by digestion with HNO_3, H_2O_2, and HCl [25], and analyzed on an ICP-MS (7700×, Agilent technologies), using rhodium as an internal standard. The blanks of the extraction and measurements were <0.2% of the lowest measured REE concentration, the reproducibility of the analysis was always better than ±5%, and spike and recovery tests showed recoveries between 94 and 106% for all REEs analyzed.

Aggregate turnover rates were calculated as in De Gryze et al. [26]., with an additional normalization step. The absolute amount of each REE in each sample should be equivalent before and after use in the experiment, but as in other REE studies, observed quantities posttreatment did not exactly match initial quantities of added REE. We therefore normalized each measured value in matrix $T_A(t)$ (see [26]):

$$\mathrm{REE}_{ni} = \frac{(\mathrm{REE}_{oi} \times \mathrm{REE}_{eTot})}{\mathrm{REE}_{oTot}},$$

where REE_{ni} are the matrix elements in $T_A(t)$ (see ref. [26]) corresponding to the normalized amount of REE (n) in each

aggregate size class (i) for each REE, REE_{oi} is the observed amount of REE in each aggregate size class for each REE, REE_{eTot} is the total initial, or expected, amount of each REE in the sample, and REE_{oTot} is the total observed amount of each REE in the sample. After completing the normalization step, we proceeded with the calculations as described in De Gryze et al. [26]. We also calculated aggregate turnover times (days) [24]. Proportion of aggregate in each size class, transformation paths, and aggregate turnover times was analyzed separately by ANOVA with presence/absence of AMF as the factor using R version 3.4.0 ([42]).

X-ray fluorescence microscopy

In order to observe spatial distributions of REEs within aggregates, we prepared thin sections of several representative aggregates from the microaggregate (53–212 µm) and small macroaggregate (212–1000 µm) size classes by mounting individual aggregates in epoxy resin and polishing them to a thickness of approximately 40 µm. Large macroaggregates were too large to provide reliable data with the X-ray fluorescence tomography technique that we intended to use, so no large macroaggregates were prepared for microscopy. These samples were then taken to the Advanced Photon Source at Argonne National Laboratory (Lemont, IL, USA) where we performed X-ray fluorescence (XRF) microscopy on the 2-ID-E beamline. During the experiment, 10.2 keV X-rays were focused onto the sample into a 0.5 µm spot, and an energy-dispersive detector recorded the spectra of fluorescence X-rays emitted by the elements in the sample. Elemental maps were generated by scanning the sample through the focal spot, and recording emitted X-ray fluorescence spectra as a function of position of the sample. Pixel size and dwell time varied with scan and details are provided in Supplementary Figures 1–8.

X-ray fluorescence data were visualized using the beamline analysis software MAPS [43]. The spectra were then fitted within the MAPS software to take account of the possible emission lines from chemical elements [44]; the position of the spectroscopic peaks depends on the emitting element and the peak area is dependent on the quantity of that element. After background correction the data were normalized to ensure that the maximum concentrations of each REE across all scans were equivalent. Rather than the highest overall value, we normalized against the median of the maximum concentrations detected in each aggregate so that any high concentration outliers would not alter the calculation. We then generated 2D images showing the location of elements across aggregates. Given the small number of aggregates scanned, we did not perform statistical analysis of the X-ray fluorescence data, and instead focused on qualitative interpretations.

The high levels of Sm seen were not unexpected since almost 42% of the soil used in the experiment was Sm labeled soil. Based on observed turnover rates for soils incubated with AMF, we expected 55.5% of soil in small macroaggregates, and 48.1% of soil in microaggregates, to be labeled with Sm. Expectations for soils incubated without AMF were similar with 55.5% of soil in small macroaggregates, and 49.2% of soil in microaggregates, to be labeled with Sm.

Data availability

Raw data for X-ray fluorescence microscopy were generated at the Advanced Photon Source at Argonne National Laboratory. Derived data supporting the findings of this study are included in the paper and its supplementary information files. Other data, REE concentrations, and aggregate size class distributions are available from the corresponding author upon reasonable request.

Acknowledgements We would like to thank Sabine Artelt and Sabine Buchert for help in the lab at FU Berlin, and the Bundesanstalt für Materialforschung und –prüfung for help preparing thin sections of soil aggregates. This research used resources of the Advanced Photon Source, a U.S. Department of Energy (DOE) Office of Science User Facility operated for the DOE Office of Science by Argonne National Laboratory under Contract No. DE-AC02-06CH11357.

Author contributions EKM, DJPM, and MCR designed the experiments. EKM and DJPM completed REE labeling and incubation. EKM, DJPM, and S-CG completed X-ray fluorescence microscopy. MB and WW completed ICP-MS work. EKM, DJPM, SV, and S-CG completed data analysis. EKM and DJPM wrote the manuscript, and all authors edited the manuscript.

Compliance with ethical standards

Conflict of interest The authors declare that they have no conflict of interest.

Publisher's note: Springer Nature remains neutral with regard to jurisdictional claims in published maps and institutional affiliations.

References

1. Hartge KH, Stewart BA. Soil structure: its development and function. Boca Raton, FL: CRC, Lewis Publishers; 1995.
2. Jastrow JD, Miller RM. Soil aggregate stabilization and carbon sequestration: feedbacks through organomineral associations. In: Lal R, Kimble JM, Follett RF, Stewart BA, editors. Soil processes and the carbon cycle. Boca Raton, FL: CRC Press; 1997. p. 207–23.
3. Miller RM, Jastrow JD. The role of mycorrhizal fungi in soil conservation. In: Bethlenfalvay GJ, Linderman RG, editors. Mycorrhizae in sustainable agriculture. Madison, WI: American Society of Agronomy; 1992. p. 29–44.
4. Oades JM. Soil organic matter and structural stability: mechanisms and implications for management. Plant Soil. 1984;76:319–37.

5. Rillig MC, Mummey DL. Mycorrhizas and soil structure. New Phytol. 2006;171:41–53.
6. Six J, Conant RT, Paul EA, Paustian K. Stabilization mechanisms of soil organic matter: implications for C-saturation of soils. Plant Soil. 2002a;241:155–76.
7. Jiménez JJ, Lal R. Mechanisms of C sequestration in soils of Latin America. CRC Crit Rev Plant Sci. 2006;25:337–65.
8. Blanco-Canqui H, Lal R. Mechanisms of carbon sequestration in soil aggregates. CRC Crit Rev Plant Sci. 2004;23:481–504.
9. Six J, Elliott ET, Paustian K, Doran JW. Aggregation and soil organic matter accumulation in cultivated and native grassland soils. Soil Sci Soc Am J. 1998;62:1367–77.
10. Wilcke W, Bol R, Amelung W. Fate of dung-applied copper in a British grassland soil. Geoderma. 2002;106:273–88.
11. von Lutzow M, Kogel-Knabner I, Ekschmitt K, Matzner E, Guggenberger G, Marschner B, et al. Stabilization of organic matter in temperate soils: mechanisms and their relevance under different soil conditions—a review. Eur J Soil Sci. 2006;57:426–45.
12. Six J, Bossuyt H, Degryze S, Denef K. A history of research on the link between (micro)aggregates, soil biota, and soil organic matter dynamics. Soil & Tillage Res. 2004;79:7–31.
13. Jastrow JD, Amonette JE, Bailey VL. Mechanisms controlling soil carbon turnover and their potential application for enhancing carbon sequestration. Clim Change. 2007;80:5–23.
14. Parwada C, Van Tol J. Effects of litter source on the dynamics of particulate organic matter fractions and rates of macroaggregate turnover in different soil horizons. Eur J Soil Sci. 2018;69: 1126–36.
15. Barto EK, Alt F, Oelmann Y, Wilcke W, Rillig MC. Contributions of biotic and abiotic factors to soil aggregation across a land use gradient. Soil Biol Biochem. 2010;42:2316–24.
16. Lehmann A, Zheng W, Rillig MC. Soil biota contributions to soil aggregation. Nat Ecol & Evol. 2017;1:1828–35.
17. Lynch JM, Bragg E. Microorganisms and soil aggregate stability. In: Stewart BA, editor. Advances in soil science. New York: Springer Verlag; 1985. p. 133–71. .
18. Bast A, Wilcke W, Graf F, Lüscher P, Gärtner H. Does mycorrhizal inoculation improve plant survival, aggregate stability, and fine root development on a coarse-grained soil in an alpine ecoengineering field experiment? J Geophys Res: Biogeosciences. 2016;121:2158–71.
19. Miller RM, Jastrow JD. Mycorrhizal fungi influence soil structure. In: Kapulnik Y, Douds DD, editors. *Arbuscular Mycorrhizae*: molecular biology and physiology. Kluwer Academic Press, Dordrecht, MA; 2000.
20. Tisdall JM, Oades JM. Organic matter and water-stable aggregates in soils. J Soil Sci. 1982;33:141–63.
21. Degens BP. Macro-aggregation of soils by biological bonding and binding mechanisms and the factors affecting these: a review. Aust J Soil Res. 1997;35:431–59.
22. Harris RF, Chesters G, Allen ON, Attoe OLJ. Mechanisms involved in soil aggregate stabilization by fungi and bacteria. Soil Sci Soc Am Proc. 1964;28:529–32.
23. Rillig M, Aguilar-Trigueros C, Bergmann J, Verbruggen E, Veresoglou S, Lehmann A. Plant root and mycorrhizal fungal traits for understanding soil aggregation. New Phytol. 2015;205:1385–8.
24. Peng X, Zhu Q, Zhang Z, Hallett P. Combined turnover of carbon and soil aggregates using rare earth oxides and isotopically labelled carbon as tracers. Soil Biol Biochem. 2017;109: 81–94.
25. Zhang XC, Friedrich JM, Nearing MA, Norton LD. Potential use of rare earth oxides as tracers for soil erosion and aggregation studies. Soil Sci Soc Am J. 2001;65:1508–15.
26. De Gryze S, Six J, Merckx R. Quantifying water-stable soil aggregate turnover and its implication for soil organic matter dynamics in a model study. Eur J Soil Sci. 2006;57:693–707.
27. Majumdar S, Peralta-Videa JR, Castillo-Michel H, Hong J, Rico CM, Gardea-Torresdey JL. Applications of synchrotron mu-XRF to study the distribution of biologically important elements in different environmental matrices: a review. Anal Chim Acta. 2012;755:1–16.
28. Paunesku T, Vogt S, Maser J, Lai B, Woloschak G. X-ray fluorescence microprobe imaging in biology and medicine. J Cell Biochem. 2006;99:1489–502.
29. Friese CF, Allen MF. The spread of VA mycorrhizal fungal hyphae in the soil: inoculum types and external hyphal architecture. Mycologia. 1991;83:409–18.
30. Tisdall JM. Possible role of soil microorganisms in aggregation of soils. Plant Soil. 1994;159:115–21.
31. Plante A, McGill W. Soil aggregate dynamics and the retention of organic matter in laboratory-incubated soil with differing simulated tillage frequencies. Soil & Tillage Res. 2002;66:79–92.
32. Hallett PD, Feeney DS, Bengough AG, Rillig MC, Scrimgeour CM, Young IM. Disentangling the impact of AM fungi versus roots on soil structure and water transport. Plant Soil. 2009;314:183–96.
33. Six J, Elliott E, Paustian K. Aggregate and soil organic matter dynamics under conventional and no-tillage systems. Soil Sci Soc Am J. 1999;63:1350–8.
34. Six J, Elliott E, Paustian K. Soil macroaggregate turnover and microaggregate formation: a mechanism for C sequestration under no-tillage agriculture. Soil Biol Biochem. 2000;32:2099–103.
35. Vogel C, Mueller C, Höschen C, Buegger F, Heister K, Schulz S, et al. Submicron structures provide preferential spots for carbon and nitrogen sequestration in soils. Nat Commun. 2014;5:2947.
36. Six J, Feller C, Denef K, Ogle SM, Sa JCD, Albrecht A. Soil organic matter, biota and aggregation in temperate and tropical soils—effects of no-tillage. Agronomie. 2002b;22:755–75.
37. Bronick CJ, Lal R. Soil structure and management: a review. Geoderma. 2005;124:3–22.
38. IUSS Working Group WRB (2014). World Reference Base for Soil Resources 2014. International soil classification system for naming soils and creating legends for soil maps. World Soil Resources Reports No. 106. Rome: FAO.
39. Vierheilig H, Coughlan A, Wyss U, Piche Y. Ink and vinegar, a simple staining technique for arbuscular-mycorrhizal fungi. Appl Environ Microbiol. 1998;64:5004–7.
40. McGonigle TP, Miller MH, Evans DG, Fairchild GL, Swan JA. A new method which gives an objective measure of colonization of roots by vesicular-arbuscular mycorrhizal fungi. New Phytol. 1990;115:495–501.
41. Sainju U. Carbon and nitrogen pools in soil aggregates separated by dry and wet sieving methods. Soil Sci. 2006;171:937–49.
42. R Core Team. R: a language and environment for statistical computing. Vienna, Austria: R Foundation for Statistical Computing; 2017.
43. Vogt S. MAPS: a set of software tools for analysis and visualization of 3D X-ray fluorescence data sets. J De Phys Iv. 2003;104:635–8.
44. Vogt S, Maser J, Jacobsen C. Data analysis for x-ray fluorescence imaging. J De Phys IV: JP. 2003;104:617–22.